Pharmaceutical aspects of subvisible particles in protein formulations

Weinbuch, D.

CHAPTER 5

MICRO-FLOW IMAGING AND RESONANT MASS MEASUREMENT (ARCHIMEDES) – COMPLEMENTARY METHODS TO QUANTITATIVELY DIFFERENTIATE PROTEIN PARTICLES AND SILICONE OIL DROPLETS

Daniel Weinbuch[1,2,*], Sarah Zölls[1,3,*], Michael Wiggenhorn[1], Wolfgang Friess[3], Gerhard Winter[3], Wim Jiskoot[2] and Andrea Hawe[1]

[1] Coriolis Pharma Research GmbH, Am Klopferspitz 19, 82152 Martinsried-Munich, Germany

[2] Division of Drug Delivery Technology, Cluster BioTherapeutics, Leiden Academic Centre for Drug Research (LACDR), Leiden University, PO Box 9502, 2300 RA Leiden, The Netherlands

[3] Department of Pharmacy, Pharmaceutical Technology and Biopharmaceutics, Ludwig Maximilian University, Butenandtstr. 5-13, 81377 Munich, Germany

* shared first authors

The chapter was published in the *Journal of Pharmaceutical Sciences: J Pharm Sci. 2013 102(7):2152-65*

Abstract

Our study aimed to comparatively evaluate Micro-Flow Imaging (MFI) and the recently introduced technique of resonant mass measurement (Archimedes, RMM) as orthogonal methods for the quantitative differentiation of silicone oil droplets and protein particles. This distinction in the submicron and micron size range is highly relevant for the development of biopharmaceuticals, in particular for products in prefilled syringes. Samples of artificially generated silicone oil droplets and protein particles were quantified individually and in defined mixtures to assess the performance of the two techniques. The built-in MFI software solution proved to be suitable to discriminate between droplets and particles for sizes above 2 µm at moderate droplet/particle ratios (70:30 – 30:70). A customized filter developed specifically for this study greatly improved the results and enabled reliable discrimination also for more extreme mixing ratios (95:5 – 15:85). RMM showed highly accurate discrimination in the size range of about 0.5 to 2 µm independent of the ratio, provided that a sufficient number of particles (> 50 counted particles) were counted. We recommend applying both techniques for a comprehensive analysis of biotherapeutics potentially containing silicone oil droplets and protein particles in the submicron and micron size range.

Introduction

Protein aggregates can be classified according to their size as visible (> 100 µm), micron (1-100 µm), submicron (100 nm-1000 nm) and nanometer particles (< 100 nm) (1). Especially aggregates in the micron and submicron size range raise concerns as they are potentially immunogenic (2,3), could coalesce to form larger particles over time or function as nuclei for further aggregation (4). Even though the United States Pharmacopeia (USP) and the European Pharmacopoeia (Ph. Eur.) currently define concentration limits in parenteral solutions only for particles larger than 10 µm, regulatory authorities increasingly expect quantitative characterization of micron particles from 1 to 10 µm and qualitative characterization of submicron particles from 100 nm to 1000 nm already in early stages of the development phase (5–7). In many cases substantial amounts of particles below 10 µm are often present in formulations that meet the limits of the pharmacopoeias for larger particles (8–10).

In general, particles of all sizes can be proteinaceous or non-proteinaceous. Among the group of non-proteinaceous particles, silicone oil droplets, which are also quantified as particles by routine methods like light obscuration, play a major role. This is especially important for products in prefilled syringes or cartridges, where silicone oil droplets are introduced into the product deriving from the lubrication of the glass barrel and the plunger. In a case study, silicone oil droplets were identified inside the eyes of patients after intravitreal injection, likely originating from the siliconized glass syringes (11). In earlier studies, silicone oil droplets were detected in insulin syringes and associated with loss of insulin efficacy (12,13). Furthermore, silicone oil droplets were present in Interferon products in prefilled syringes (14). Even though silicone oil itself is not necessarily harmful to the patient (15), it has been described to induce aggregation of monoclonal antibodies (16) and various other proteins (17,18), and the formation of protein-silicone oil complexes (18,19), which might potentially be immunogenic (20). From a manufacturing perspective, elevated concentrations of (silicone) oil droplets can indicate problems during the production process, e.g., improper siliconization of syringes or contamination from leaking components during lyophilization. These factors make an analytical differentiation of the total particle load into protein particles and silicone oil droplets necessary.

Among the various techniques for particle analysis (21), scanning electron microscopy coupled with energy dispersive X-ray spectroscopy (SEM-EDX) (22), Fourier-transformed infrared (FTIR) (22), and Raman microscopy (23), asymmetrical flow field flow fractionation (24), electrical sensing zone as well as flow cytometry (25) are in principle able to differentiate silicone oil droplets and protein particles. However, mainly flow

imaging microscopy techniques and the recently introduced resonant mass measurement (RMM) technique are designed for the differentiation of these particles in a higher throughput and without cumbersome sample preparation (e.g. staining or fixation). Micro-Flow Imaging (MFI) has received major attention for the analysis of protein particles (22,26–28) but has also been applied for the identification of silicone oil droplets (29). Silicone oil droplets were successfully differentiated from protein particles on MFI images on the basis of their spherical shape (30) and, more efficiently, by employing a multi-parametric filter (31).

The recently introduced Archimedes system employs the novel principle of RMM for the analysis of submicron and micron particles (32). The sample solution is flushed through a microchannel inside a resonating cantilever (also designated as suspended microchannel resonator (SMR)) which changes its frequency depending on the mass of the particles passing the channel. Importantly, positively buoyant particles (e.g. silicone oil droplets) and negatively buoyant particles (e.g. protein particles) can be clearly discriminated as they increase and decrease the frequency of the cantilever, respectively (33). With a theoretical size range from about 50 nm up to about 6 µm (depending on the sensor and the particle type), RMM bridges the "submicron size gap" (15,34) between on the one hand flow imaging microscopy and light obscuration, which cover the micrometer size range, and on the other hand nanoparticle tracking analysis and dynamic light scattering, which allow analysis in the nanometer size range. Literature on RMM is still very limited. Patel et al. (35) presented a first study on the principle of RMM using various microspheres as well as silicone oil droplets and protein particles for a technical evaluation of the system. Barnard et al. (14) applied RMM to analyze protein particles and silicone oil droplets in marketed Interferon-beta products. However, the accuracy of the differentiation between these two particle types was not investigated in those studies and remains to be elucidated.

The aim of our study was to evaluate MFI and RMM as orthogonal tools for the quantitative discrimination between silicone oil droplets and proteinaceous particles in the micron and submicron range. For this purpose, defined mixtures of silicone oil droplets and protein particles were prepared at various ratios on the basis of the distributions expected in marketed biopharmaceutical products in prefilled syringes. The optical discrimination of silicone oil droplets from protein particles in MFI by (i) the built-in software solution "find similar" and (ii) a new customized data filter developed in this study was compared to the physical discrimination principle of RMM.

Materials & Methods

Materials

Etanercept (Enbrel®, prefilled syringe, lot no. 31576, exp. 12/2008; lot no. 32411, exp. 09/2009), adalimumab (Humira®, prefilled syringe, lot no. 292209A05, exp. 10/2006; lot no. 430989A04, exp. 02/2008), rituximab (MabThera®, vial, lot no. B6073, exp. 12/2013), and infliximab (Remicade®, vial, lot no. 7GD9301402, 7FD8701601, 7RMKA81402, pooled) were donated by local hospitals. Sucrose, mannitol, sodium chloride, trisodium citrate dihydrate and polysorbate 80 were purchased from VWR (Darmstadt, Germany), disodium hydrogenphosphate dihydrate and sodium dihydrogenphosphate dihydrate were purchased from Merck KGaA (Darmstadt, Germany). Silicone oil with a viscosity of 1000 cSt (same viscosity as used in other studies (15,16,25) and as listed in the Ph.Eur. monography for silicone oil as a lubricant (36)), citric acid, and arginine hydrochloride were purchased from Sigma Aldrich (Steinheim, Germany).

Preparation of protein samples

Etanercept solution at a concentration of 5 mg/mL was prepared by dilution of 50 mg/mL etanercept (removed from the prefilled syringe through the needle) in 25 mM phosphate buffer (pH 6.3) containing 100 mM NaCl, 25 mM arginine hydrochloride, and 1% sucrose. Adalimumab solution at a concentration of 5 mg/mL was prepared by dilution of 50 mg/mL adalimumab in 15 mM phosphate/citrate buffer (pH 5.2) containing 105 mM NaCl, 1.2% mannitol, and 0.1% polysorbate 80.

Rituximab solution at a concentration of 1 mg/mL was prepared by dilution of 10 mg/mL rituximab commercial product in 25 mM citrate buffer (pH 6.5) containing 154 mM NaCl and 0.07% polysorbate 80 (formulation buffer). The formulation was filtered using a 0.2-µm polyethersulfone syringe filter (Sartorius, Göttingen, Germany) and kept at 2-8 °C for a maximum of one week. Heat-stressed rituximab was prepared by incubating 1.5 mL of the 1 mg/ml rituximab solution for 30 min at 71 °C in a thermomixer (Eppendorf, Hamburg, Germany). Stir-stressed rituximab was prepared by incubating 3 mL of the 1 mg/ml rituximab solution in a 5R glass vial using a 12 mm Teflon®-coated stir bar at 1000 rpm for 24 hours at room temperature on a magnetic stirrer (Heidolph MR 3001K, Heidolph, Schwabach, Germany). Stressed rituximab at 1 mg/ml (protein particle stock suspension) was stored at 2-8°C until the measurement.

Infliximab solution at a concentration of 1 mg/mL was prepared by dilution of 10 mg/mL infliximab commercial product in 100 mM phosphate buffer (pH 7.2). The formulation was filtered using a 0.2-µm polyethersulfone syringe filter. Heat-stressed infliximab was

prepared by incubating 0.5 mL of the 1 mg/mL infliximab solution for 30 minutes at 60 °C in a thermomixer. Stir-stressed infliximab was prepared by incubating 8 mL of the 1 mg/mL infliximab solution in a 10R glass vial using an 18-mm Teflon®-coated stir bar at 250 rpm for 24 hours at room temperature on a magnetic stirrer (Heidolph MR Hei-Standard).

Preparation of silicone oil emulsion

Pure silicone oil was added to filtered formulation buffer (0.2-µm polyethersulfone syringe filter (Sartorius, Göttingen, Germany)) in a particle-free 15-mL conical tube (VWR, Darmstadt, Germany) to a final concentration of 2% (w/v) to generate a pure emulsion without additives. After vortexing briefly, silicone oil droplet formation was induced by sonication in a water bath (Sonorex, Brandelin, Berlin, Germany) for 10 min. Fresh silicone oil emulsion (silicone oil droplet stock emulsion) was prepared on the day of the measurement and kept at room temperature.

Preparation of individual and mixed samples of silicone oil droplets and protein particles

Silicone oil droplet stock emulsion and/or protein particle stock suspension (heat-stressed rituximab) was diluted in unstressed protein solution or filtered formulation buffer for the preparation of mixed and individual samples. Unless stated otherwise, samples were prepared to a final protein concentration of 0.5 mg/mL. Mixed samples were prepared to cover ratios of silicone oil droplets to protein particles of 95:5 to 15:85 based on particle counts > 1 µm determined by MFI. Individual samples were prepared to contain the same amount of silicone oil droplets and protein particles, respectively, as in the mixed samples and were referred to as the theoretical concentration. The samples were gently mixed with a pipette, kept at room temperature and measured on the day of preparation.

Micro-Flow Imaging

An MFI DPA4100 series A system (ProteinSimple, Santa Clara, California) equipped with a 100-µm flow cell, operated at high magnification (14x) and controlled by the MFI View software version 6.9 was used. The system was flushed with 5 mL purified water at maximum flow rate and flow cell cleanliness was checked between measurements. Unstressed and filtered rituximab or the appropriate formulation buffer was used to perform “optimize illumination” prior to each measurement. Samples of 0.65 mL with a pre-run volume of 0.3 mL were analyzed at a flow rate of 0.1 mL/min (n=3). MVAS version 1.2 was used for data analysis.

Development of a customized filter for MFI

The MVAS software of the MFI system enables the discrimination of particles based on optical parameters of the generated images through the "find similar" operation. For our study, a minimum of 20 particles above 5 µm clearly recognizable as silicone oil droplets was selected for the discrimination. In addition to this, a customized filter was developed specifically for the heat-stressed Rituximab samples of this study. In detail, the new filter was based on four customized size-specific cut-offs for particle parameters of silicone oil droplets provided by MFI (Figure 1), which proved to be suitable to discriminate silicone oil droplets and protein particles. This approach is a modification of previous work by Strehl et al. (31). The four parameters used for our filter were intensity mean (Figure 1A), intensity minimum (Figure 1B), intensity standard deviation (Figure 1C) and aspect ratio (Figure 1D).

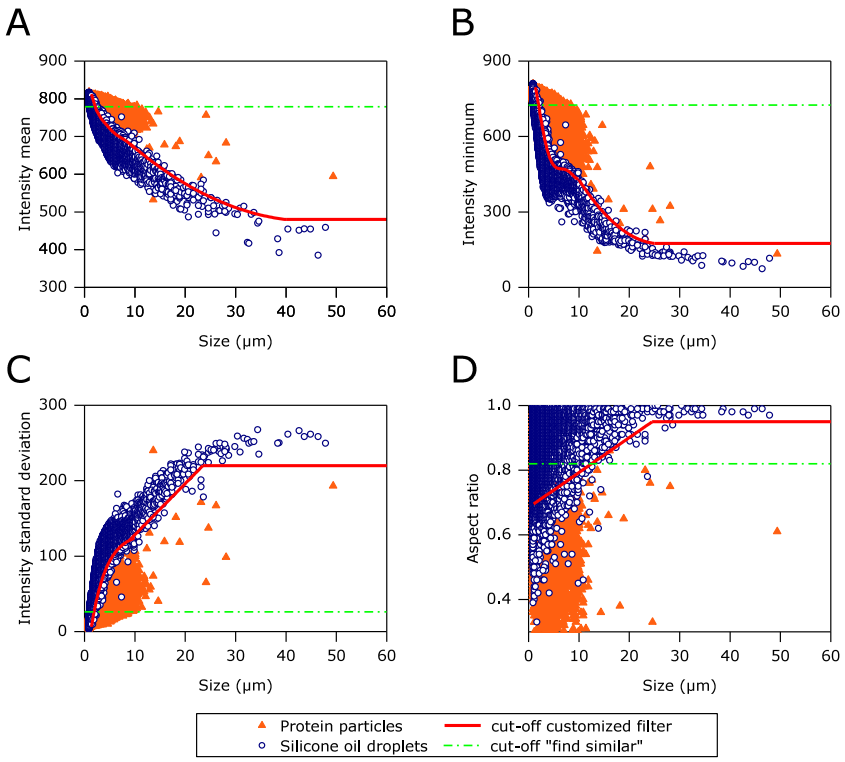

Figure 1 Scatter plots of particle parameters: A) intensity mean, B) intensity minimum, C) intensity standard deviation, and D) aspect ratio for individual samples containing only protein particles (heat-stressed rituximab) or only silicone oil droplets analyzed separately by MFI and merged into one graph per particle parameter. The solid red lines illustrate cutoffs as a function of size, generated by our customized fit for the discrimination between silicone oil droplets and protein particles. The dash-dotted green lines illustrate linear cutoffs used by the MVAS software for the "find similar" operation.

The first three parameters are based on the intensity of the particle image, which is directly proportional to the transparency of the particle (27). The intensity mean describes the mean intensity value over all pixels within one particle; the intensity minimum describes the intensity of the darkest pixel of a particle; and the intensity standard deviation describes differences between higher and lower intensity values within the same particle. The aspect ratio defines the shape of a particle with "1" for an absolutely spherical particle and "0" for a needle with an infinite length. For each of the four particle parameters, the individual distributions for silicone oil droplets and protein particles from heat-stressed rituximab were compared as a function of size. Cut-offs were defined at the mean value of the 95% confidence intervals between the two populations (Figure S1). A polynomial function was automatically fitted to these points from 1 to 11 µm and applied for particles from 1 to 9 µm. Above 11 µm, the number of counts acquired was not sufficient for this statistical approach; therefore, the fit was adjusted manually in this larger size range. The automated and the manual fit were overlapped in the size range from 9 to 11 µm to ensure a smooth transition. Since the silicone oil droplet population was more homogeneous than the protein particle population, the customized filter was set to identify objects as silicone oil droplets only when they fulfilled all four cut-off fit criteria. Particles showing values below the cutoff for intensity mean and minimum (Figure 1A and B) and at the same time above the cutoff for intensity standard deviation and aspect ratio (Figure 1C and D) were marked as silicone oil droplets by the algorithm. Particles fulfilling less than four of these criteria were assigned as non-silicone oil particles, which means in our case protein particles.

Resonant mass measurement

An Archimedes system (Affinity Biosensors, Santa Barbara, California) was equipped with a Hi-Q Micro Sensor and controlled by ParticleLab software version 1.8. The sensor was flushed for 60 s with purified water prior to analysis. Subsequently, possible impurities in the system were removed by two "sneeze" operations (liquid in the sensor is pushed into both directions) and the system was flushed again for 60 s with purified water. The sample solution was then loaded for 45 s. Prior to analysis, the limit of detection (LOD) was determined three times in automatic LOD mode. The mean value was then set fixed for each measurement. Samples of 150 nL were analyzed (n=3) and fresh sample solution was loaded for each of the triplicate measurements.

Size determination of particles by RMM is based on the frequency shift f which is proportional to the buoyant mass M_B and depending on the sensitivity S of the resonator (Equation 1).

$$M_B = \Delta f * S$$

Equation 1

The conversion of buoyant mass M_B into dry mass M (Equation 2) and diameter D (Equation 3) is then based on the density of the particle, $\rho_{particle}$ (1.32 g/mL for protein particles, based on the density of pure protein (37) and the recommendation of the manufacturer; 0.97 g/mL for silicone oil, according to the supplier) and the density of the fluid, ρ_{fluid} (calculated based on the sensor frequency relative to the frequency and the density of water as a reference).

$$M = \frac{M_B}{1 - \rho_{fluid} / \rho_{particle}}$$

Equation 2

$$D = \sqrt[3]{\frac{6M}{\pi \rho_{particle}}}$$

Equation 3

Results and discussion

Silicone oil droplets in prefilled syringes

Expired prefilled syringes of etanercept and adalimumab were available for the study and analyzed in order to gain insight into relevant levels and size distributions of silicone oil droplets in marketed products as a worst case scenario. Four and six years after expiration, respectively, MFI determined for both products about $4x10^5$ particles/mL above 1 µm. Based on the images generated by MFI, about 80% of the particles above 5 µm in both products could be identified as silicone oil droplets using the "find similar" operation provided by the MVAS software. RMM determined $3.2x10^6$ particles/mL larger than 0.5 µm for etanercept and $2.0x10^6$ particles/mL for Adalimumab, of which 51% and 97%, respectively, could be attributed to silicone oil. Three and four years after expiration, RMM determined for both analyzed products lower concentrations of protein particles and of silicone oil droplets when compared to products four and six years after expiration, respectively (Table S1). This implies that total particle concentrations as well as the ratio between silicone oil droplets and protein particles can vary substantially between products, lots and age of the product.

Determination of total particle concentrations (without discrimination)

For the evaluation of MFI and RMM, silicone oil droplets were artificially generated, which appeared similar to those found in etanercept and adalimumab prefilled syringes with respect to their shape, optical properties (Figure 2) and size distribution (Figure S2). The concentrations used in our study (0.003% to 0.025% (w/v) silicone oil) provided droplet concentrations similar to those identified in the expired etanercept and adalimumab prefilled syringes and are in agreement with other studies suggesting the presence of up to 0.03% of silicone oil in prefilled syringes (38,39). A heat-stress method was developed using rituximab as a model for the generation of particles with a similar appearance to protein particles in etanercept prefilled syringes. A stir-stress method was developed for the generation of particles similar to those in adalimumab prefilled syringes (Figure 2). All protein samples showed comparable particle size distributions with the smaller particles representing the largest fraction (Figure S3). Protein particles in concentrations from $1x10^5$ to $5x10^5$ particles/mL above 1 µm (according to MFI) were combined with silicone oil droplets in concentrations from $1x10^5$ to $3x10^5$ particles/mL above 1 µm (according to MFI). Using MFI and RMM, several samples with varying concentrations of protein particles and silicone oil droplets were analyzed, both individually and as mixtures at various defined droplet/particle ratios.

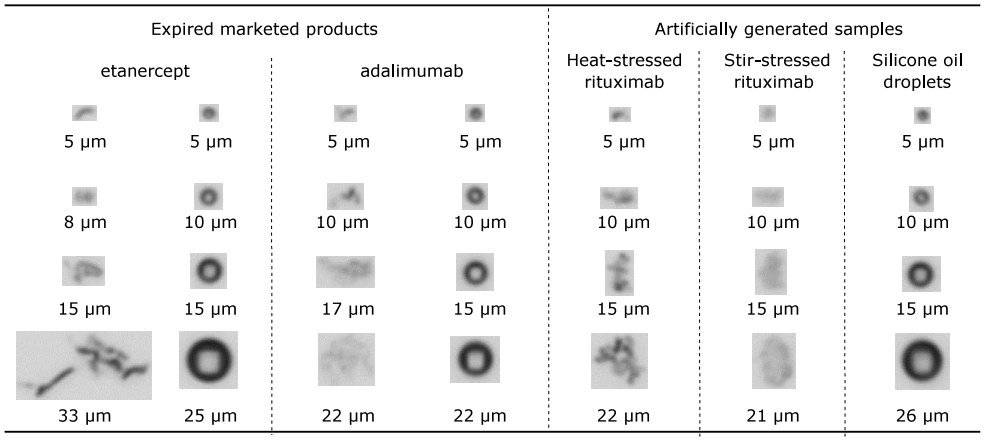

Figure 2: Examples of MFI images of protein particles and silicone oil droplets detected in marketed products and artificially generated samples.

First, the particle concentrations for individual samples containing either only silicone oil droplets or only protein particles were determined by MFI and RMM. One combination is shown as a representative example in Figure 3 for the overlapping measurement size range of both techniques (1-4 µm). Overall, the results indicate that particle counts and size distributions by MFI and RMM are in general agreement. However, certain differences

were observed depending on the type of sample and the ratio of protein particles and silicone oil droplets: For samples containing only silicone oil, RMM detected slightly more droplets of 1 to 4 µm as compared to MFI, while MFI detected more droplets in the size range from 2 to 4 µm (Figure 3A). This trend was reproducible for all silicone oil droplet samples, with an up to twofold higher silicone oil droplet count in the size range of 1 to 4 µm detected by RMM as compared to MFI.

This difference might be due to two major reasons:

(i) Silicone oil droplets of sizes up to 50 µm were identified by MFI, which are much larger than the microchannel diameter of RMM (8 µm). Those particles larger than 8 µm represent only 4% of all silicone oil droplets in the sample detected by MFI by number; however, they contain 72% of the total mass of all silicone oil droplets in the sample detected by MFI (mass was calculated based on droplet counts at the respective diameter and the density of silicone oil of 0.97 g/mL). These observations led us to the hypothesis that larger silicone oil droplets might be fragmented into smaller ones by shear forces inside the microchannels and capillaries of the RMM system. This would result in an increased number of smaller silicone oil droplets in RMM. Our hypothesis was supported by MFI data from a sample containing only silicone oil, which was analyzed before RMM and collected after an RMM measurement. In this case, an increase in silicone oil droplet concentration between 1 and 2 µm with a concomitant decrease above 2 µm was observed when comparing particle concentrations before and after the RMM measurement (Figure S4A). It could be shown that this was clearly an effect of the RMM measurement itself and not of the dilution of the sample during the RMM measurement (Figure S4B). A decreased flow rate during sample analysis might reduce this fragmentation effect but would further increase the already long measurement time of RMM.

(ii) Additionally, small particles near the detection limit of MFI could be “overlooked” by the software, as suggested also by others (40), further enhancing the differences between MFI and RMM for small (1 µm) silicone oil droplet counts.

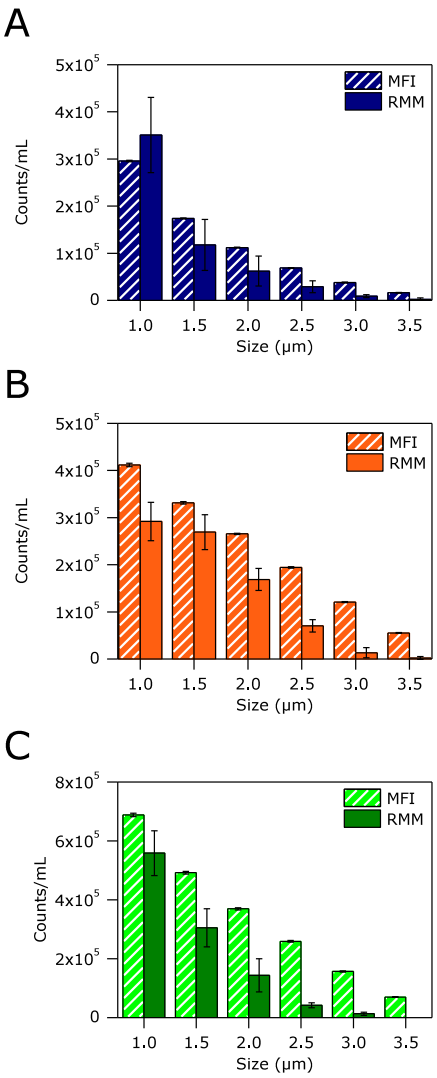

Figure 3: Cumulative counts in the size range of 1–4 µm of A) a sample containing only silicone oil droplets, B) a sample containing only protein particles (heat-stressed rituximab), and C) the corresponding mixture (droplet–particle ratio 40:60 for particles >1 µm based on MFI) as determined by MFI and RMM. Error bars represent standard deviations from triplicate measurements.

In contrast to the results from silicone oil samples, RMM detected consistently less protein particles in individual samples than MFI over the entire 1 to 4 µm size range (Figure 3B). This was also observed in a previous study by our group (41). This difference is suggested to occur for two reasons:

(i) MFI and RMM apply fundamentally different measurement principles (Figure 4): MFI captures 2D microscopic particle images (Figure 4A) and size determination of particles by MFI is performed according to their spatial dimension on the images defined by the outer boundary of the particle. The differentiation of protein particles and silicone oil droplets is based on morphological parameters such as particle shape and transparency. In contrast, RMM detects particles as distinct positive or negative peaks in the frequency trace caused by the physical parameter of particle buoyancy (Figure 4B). However, protein particles may vary in density and contain substantial amounts of liquid (42). This is not included into the size calculation by RMM, causing a potential underestimation of particle sizes in RMM as compared to MFI, which includes liquid inside the particle in the size calculation. This in turn would lead to an apparent shift of the complete particle size distribution in RMM towards smaller particle sizes resulting in lower concentrations detected for the respective size bins in RMM as compared to MFI.

(ii) As a second reason, the micron-sized capillaries and channels of the RMM sensor are vulnerable to clogging by particles at or above the upper size limit of the system. Even though RMM offers several tools to remove stuck particles, clogging cannot always be avoided. Thus, large stuck particles could hinder other particles from reaching the sensor. This could explain why the concentration discrepancy between RMM and MFI is more pronounced at larger particle sizes. Smaller particles will pass a clogged site more easily, whereas larger particles, although still in the measurement range, are more likely to be excluded from the analysis. Altogether, this will result in lower apparent protein particle concentrations in RMM. A possible solution would be sample preparation for highly aggregated samples, e.g. filtration or centrifugation, which can however potentially change sample properties. In the future, a potential system reconfiguration by the manufacturer could decrease clogging issues.

Total particle concentrations for mixed samples containing both silicone oil droplets and protein particles also revealed slight differences between MFI and RMM for the overlapping size range of 1 to 4 µm (Figure 3C). For moderate ratios (silicone oil droplets/protein particles 40:60 based on MFI shown as a representative sample), RMM detected less particles than MFI, likely due to the underestimation of protein particles as described before. However, in mixed samples of higher silicone oil content (silicone oil droplets/protein particles 80:20 or 95:5 based on MFI) similar concentrations were determined by the two techniques. In those samples, the overestimation of silicone oil droplets by RMM was balanced out by the underestimation of protein particles by RMM leading to similar total particle counts in MFI and RMM. For all samples, RMM showed

higher standard deviations than MFI. This is probably mainly due to the small analyzed volume in RMM (about 0.15 µL) as compared to MFI (about 35 µL).

It was further investigated whether the presence of both silicone oil droplets and protein particles within the same sample influenced the accuracy of MFI or RMM to determine total particle concentrations. For MFI, the concentration determined for mixed samples of silicone oil droplets and protein particles from heat-stressed rituximab matched very closely the sum of the concentrations determined for the corresponding individual samples (Figure S5A). For RMM, the concentration for the mixed sample reasonably matched the sum of the individual samples for the main size classes (Figure S5B). These observations were consistent for different ratios and also for protein particles from stir-stressed rituximab mixed with silicone oil droplets. This justified the use of particle counts of individual samples as the theoretical concentrations for mixed samples.

Discrimination between silicone oil droplets and protein particles

The discrimination between silicone oil droplets and protein particles by MFI and RMM is based on clearly different mechanisms (see above and Figure 4). The optical discrimination by MFI bears the potential risk of false classification due to optically similar silicone oil droplets and protein particles in the lower size range, especially near the detection limit. In contrast, the discrimination by RMM based on the physical parameter of particle buoyancy enables a clear discrimination with minimal risk of false classification. In this case, the difference in density between silicone oil droplets and protein particles is beneficial.

Discrimination between droplets and particles by MFI

In the present paper, the performance of MFI was assessed using the built-in software solution "find similar" and a customized data filter developed specifically for this study. To evaluate the reliability of our customized filter, the following control experiments were performed: the filter was applied on samples containing only silicone oil droplets and the number of objects falsely marked as protein particles was determined and vice versa. Our customized filter marked less than 3% of the counts in the samples containing only silicone oil droplets ($3x10^5$ particles/mL > 1 µm based on MFI) falsely as protein particles (> 2 µm) and less than 8% of the counts in the samples containing only protein particles ($4x10^5$ particles/mL > 1 µm based on MFI) falsely as silicone oil droplets (> 2 µm). These controls illustrate the capability of our filter to properly discriminate protein particles and silicone oil droplets. The requirement that all four criteria of particle parameters need to be fulfilled at the same time is the main difference of our filter compared to the filter

previously developed by Strehl et al. (31), which used the product of four particle parameters as criterion for particle classification. In this case, extreme values in one parameter could shift the product to the side of one particle type although the other three parameters would classify it clearly as the other particle type. Thus, their filter led to errors of 10% to 12% (> 2 µm) for silicone oil droplets classified falsely as protein particles; the error for protein particles classified falsely as silicone oil droplets depended strongly on the type of protein particles and varied between 2% and 42% in their study (31).

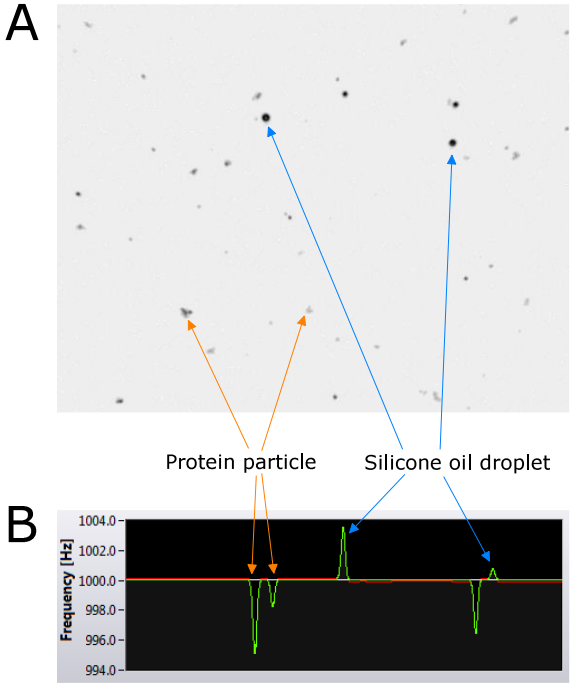

Figure 4: aw data of an exemplary mixed sample containing protein particles (heat-stressed rituximab) and silicone oil droplets from A) MFI (image-based discrimination) and B) RMM (frequency-based discrimination).

In contrast, our filter applies more strict criteria for silicone oil droplet identification as particles fulfilling only three out of four criteria are not marked as silicone oil droplets leading to lower errors as discussed above. However, for protein particles generated from a different monoclonal IgG (infliximab) by heat stress or stir stress the customized filter marked up to 40% (> 2 µm) falsely as silicone oil droplets. This was most likely due to the lower intensity (lower transparency) of particle images of this IgG, which makes a misclassification as silicone oil droplets of similarly low transparency more likely. This is in agreement with the literature, where large variations were also observed by Strehl et al. (31) when their filter was applied to different types of protein particles. The MVAS

software filter could not be tested on these protein samples as it was based on manual selection of silicone oil droplet images which were not present in these pure protein samples.

The “find similar” operation of the MVAS software as well as the customized filter were both used to categorize particles from mixed samples into silicone oil droplets and non-silicone oil particles. Non-silicone oil particles were defined as protein particles in our case. The obtained concentrations were compared to the theoretical concentrations based on the analysis of the individual samples, which were used to assess the accuracy of both methods (Figure 5A, C, and Figure 6). For moderate droplet/particle number ratios from 30:70 to 70:30 based on MFI, both the selection by “find similar” and the customized filter were able to determine the correct concentrations within acceptable deviations for particles > 2 µm. This was observed for samples containing silicone oil droplets and protein particles from heat-stressed Rituximab (Figure 5A exemplarily shows the results for a sample with a droplet/particle ratio of 40:60 based on MFI). For stir-stressed Rituximab (Figure 5C) the customized filter for MFI showed superior discrimination compared to the “find similar” method for particles > 2 µm, even though the customized filter was designed based on heat-stressed Rituximab particles. The even higher intensity of MFI particle images of stir-stressed Rituximab compared to those of heat-stressed Rituximab (Figure 2) likely contributes to this: since three out of four parameters of the customized filter are based on the particle intensity, it facilitates discrimination from the lower intensity silicone oil droplets. Furthermore, the customized filter was superior for samples with more extreme droplet/particle number ratios (see Figure 6A and B for representative examples) and for samples based on original, undiluted Rituximab solution (Figure 6C).

Thus, for particles between 2 µm and 25 µm, the development of a customized filter is useful for an accurate discrimination by MFI. For particles with a size below 2 µm, discrimination by an alternative method is recommended (e.g. RMM, as discussed later) as both “find similar” and the customized filter were not reliably capable of determining the correct concentration. For particles larger than 25 µm, due to usually low particle numbers in this size range, manual classification of the MFI images might be preferred over the built-in software solution or a customized filter. Those particles can usually be identified easily by visual evaluation of the images.

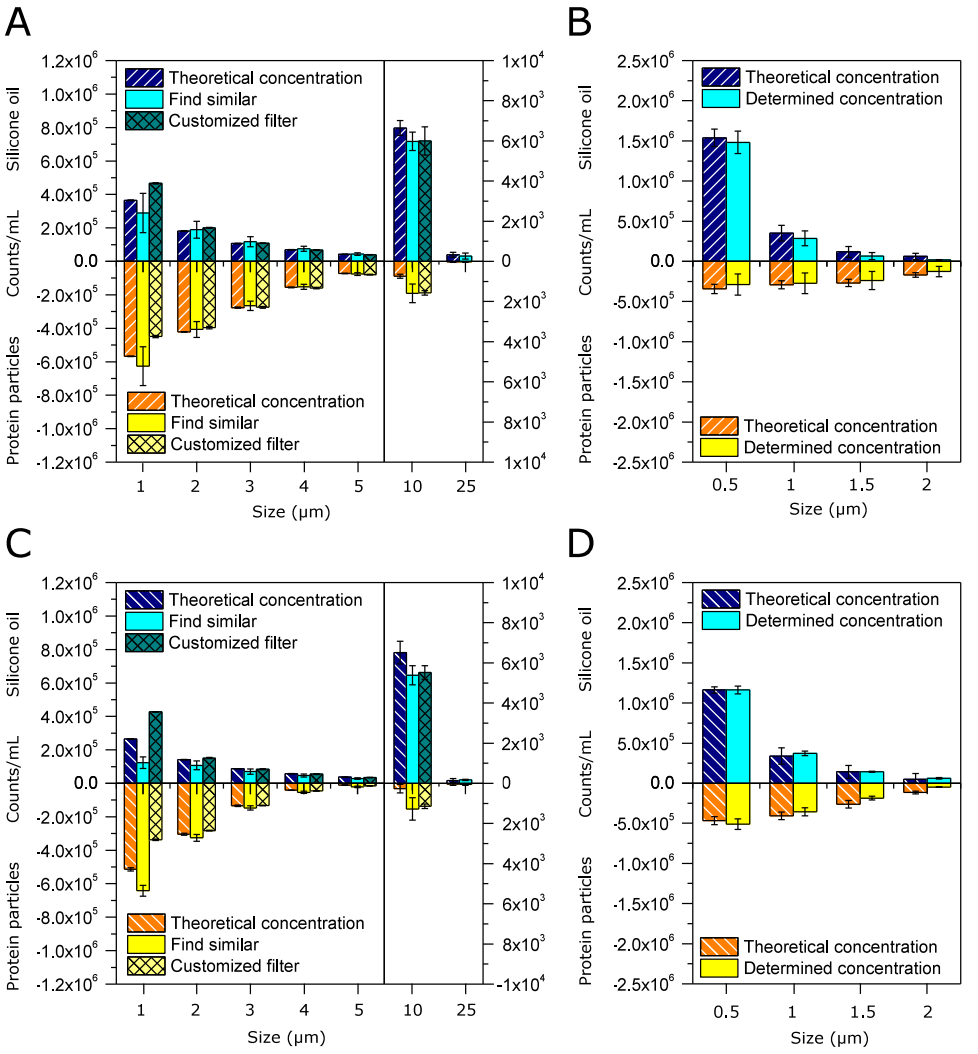

Figure 5: Results from MFI (A and C) or RMM (B and D) for the discrimination between silicone oil droplets and protein particles. Histograms comparing the theoretical concentrations (based on individual samples) and determined concentrations of silicone oil droplets and protein particles (A and B, heat-stressed rituximab; C and D, stir-stressed rituximab) in mixed samples with moderate ratios (droplet–particle ratio 40:60 based on MFI). Error bars represent standard deviations from triplicate measurements.

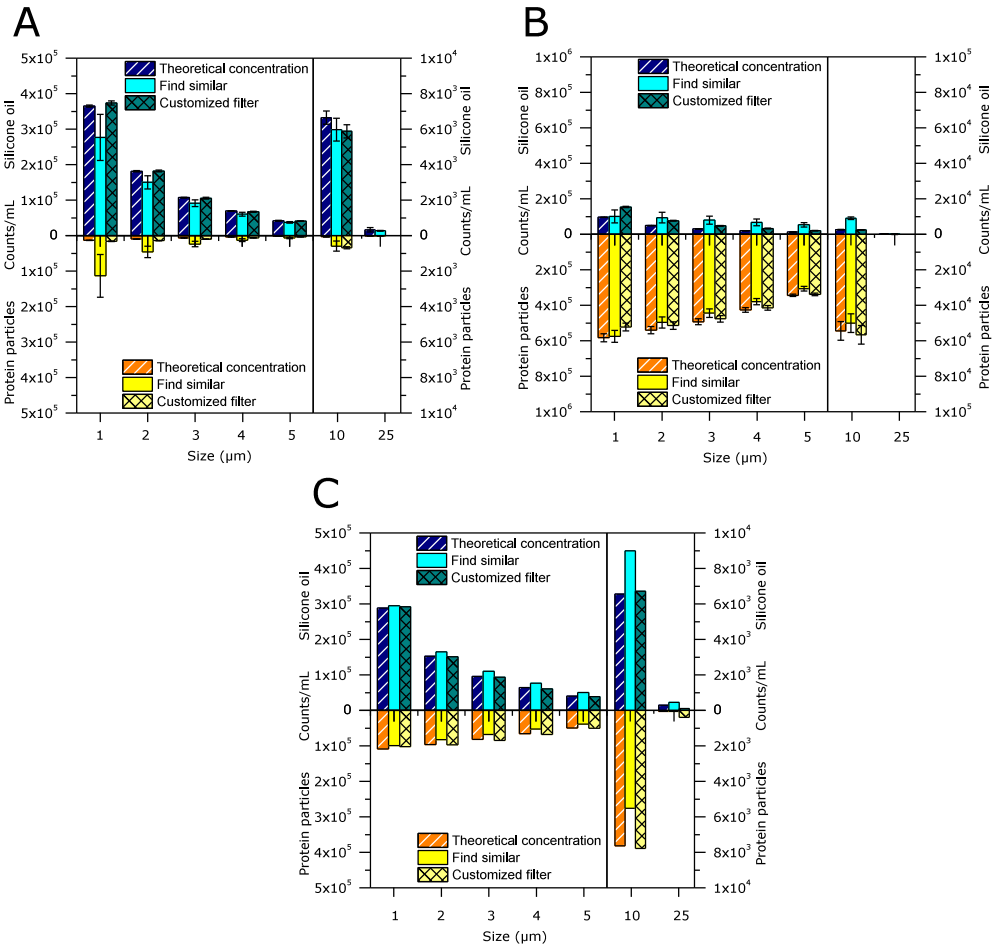

Figure 6: MFI cumulative particle counts comparing theoretical concentrations (based on individual samples) and determined concentrations of silicone oil droplets and protein particles (heat-stressed rituximab) in droplet–particle ratios of A) 95:5 and B) 15:85 in samples containing 0.5 mg/mL rituximab as well as C) 60:40 in a sample containing undiluted rituximab (10 mg/mL). Error bars (A and B) represent standard deviations from triplicate measurements.

Discrimination between droplets and particles by RMM

As described for MFI, RMM was evaluated with respect to an accurate discrimination between silicone oil droplets and protein particles in mixed samples (Figure 5B, D, and Figure 7). For moderate particle/droplet ratios, RMM was consistently able to discriminate particles correctly with small deviations from the theoretical concentrations for heat-stressed (Figure 5B) and stir-stressed rituximab (Figure 5D). Large deviations of 20% or more from the theoretical concentration were only observed if the discrimination was

based on less than 50 counted particles (corresponding in this case to total concentrations (droplets + particles) < $3x10^5$ particles/mL) and thus statistical representation of the sample population was limited. This was for example the case for particles larger than 2 µm (Figure 5B and D). Increasing the analyzed sample volume would compensate for the limited reliability of RMM to quantify low particle concentrations, as also reported by others.35 However, it needs to be considered that very long measurement times associated with large analyzed volumes could also provoke changes in sample properties. In contrast, fairly high concentrations of protein particles > $2x10^6$ particles/mL caused high standard deviations potentially due to the increased probability of coinciding particles and also blockage of the channel by particles (Figure 7A). However, extreme droplet/particle ratios with high amounts of silicone oil droplets provided moderate standard deviations and also fairly accurate determination of the theoretical concentration (Figure 7B exemplarily displays results for a droplet/particle ratio of 95:5 based on RMM). Those results provide evidence that RMM discrimination is reliable for particles below 2 µm.

Comparison of results for MFI and RMM

For a final evaluation of MFI and RMM regarding the discrimination of silicone oil droplets and protein particles, results for the same sample were compared between the two techniques. For silicone oil droplets and heat-stressed Rituximab (Figure 5A and B, droplet/particle ratio 40:60) as well as stir-stressed Rituximab (Figure 5C and D, droplet/particle ratio 40:60), RMM detected a higher fraction of silicone oil droplets as compared to MFI for the sizes above 1 µm already in the individual samples. This originated foremost from the differences in total concentration determination as discussed earlier: RMM detected in general more silicone oil droplets than MFI, whereas MFI detected in general more protein particles than RMM (see also Figure 3). However, in this size range, RMM results for the mixed samples are considered more reliable as RMM differentiation was shown to be highly accurate (Figure 5B and D). MFI differentiation suffered from low image resolution in the lower size range leading to large deviations for both the “find similar” operation and the customized filter (Figure 5A and C). With increasing particle size, the ratios between MFI and RMM in the individual samples converged and similar ratios for individual samples were obtained for particles > 2 µm (Figure 5A and B show a droplet/particle ratio of 30:70 for particles > 2 µm in individual samples for both MFI and RMM). For mixed samples, the concentration obtained by MFI is suggested to be more reliable for sizes above 2 µm as the discrimination between droplets and particles was highly accurate, especially when the customized filter was applied (Figure 5A and C). RMM analysis of objects with a size above 2 µm was based on small

numbers of counts, questioning the reliability of the determined concentrations (Figure 5B and D) in our study.

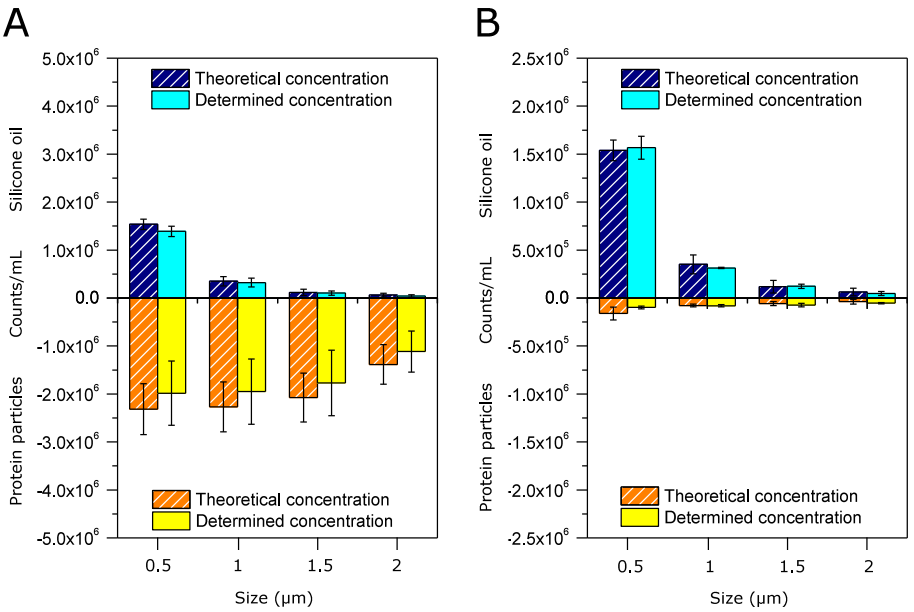

Figure 7: RMM cumulative particle counts comparing theoretical concentrations (based on individual samples) and determined concentrations of silicone oil droplets and protein particles (heat-stressed rituximab) in droplet–particle ratios of A) 40:60 and B) 95:5. Error bars represent standard deviations from triplicate measurements.

Recommendations and conclusions

Table 1 summarizes properties as well as pros and cons during the application of MFI and RMM which were identified in our study. For MFI, the customized filter was shown to provide correct results for moderate and extreme ratios between silicone oil droplets and protein particles. The filter was developed using heat-stressed rituximab particles, but was also found applicable for rituximab particles generated by stir stress and for samples containing rituximab solution in high concentrations (10 mg/mL). In contrast, the application for infliximab particles generated by either heat or stir stress resulted in large errors. These results emphasize the necessity of customizing the filter to each specific protein, the formulation, and the particle type / stress method of interest. Thus, the development of a customized filter for quality control of protein therapeutics in prefilled syringes with comparable manufacturing conditions can be considered reasonable. In contrast, the implementation during formulation development with varying conditions should be critically evaluated case by case. The separation by the MVAS software was

acceptably accurate especially for moderate ratios of silicone oil droplets and protein particles. It could still be applied in those cases, when costs and time for the development of a customized filter would exceed the benefit of a more accurate discrimination. However, the differentiation by "find similar" showed clearly higher standard deviations as compared to the customized filter. This higher variation of the "find similar" operation originated most likely from the underlying sample and operator dependent manual selection of the particle images. For both MFI-based solutions it is important to consider that the separation is based on the identification of silicone oil droplets, whereas the remaining particles, identified only as "non-silicone oil particles", are simply equated with protein particles by the operator.

Table 1: Summarizing comparison of MFI and RMM for the analysis of silicone oil droplets and protein particles.

	MFI (MFI4100, HighMag Settings)	**RMM (Archimedes, Micro Sensor)**
Properties of the techniques		
Principle	Flow imaging microscopy with digital image analysis. Sizing based on optical particle boundary.	Mass determination by quantification of frequency shift. Sizing based on particle density
Size range	1-70 µm	0.3-4 µm
Differentiation of protein particles and silicone oil droplets	Based on morphological parameters (shape, transparency…) of particle images. Differentiation may be time-consuming (esp. development of customized filter).	Based on particle buoyancy (density). Differentiation during the measurement without additional time consumption.
Concentration range	Up to $1x10^6$ particles/mL (coincidence not indicated by the system)	$3x10^5$ to $1x10^7$ particles/mL (coincidence indicated by the system)
Reproducibility	Higher reproducibility	Lower reproducibility (due to lower analyzed volume)
Status of the technique	Established R&D and cGMP technique	Novel R&D technique
Pros and Cons during application		
Protein particles	Clear visualization of larger particles.	Clogging by larger particles possible.
Silicone oil droplets	Detection of larger droplets without fragmentation.	Fragmentation of larger droplets possible.
Samples containing protein particles and silicone oil droplets	2-10 µm: good differentiation by built-in software filter or (preferably) customized filter. > 10 µm: easy identification by optical evaluation of particle images.	0.5-2 µm: unambiguous differentiation due to physical detection principle.
Complexes of protein particles and silicone oil droplets	Potential identification of larger complexes (> about 5-10 µm).	Potential misclassification, miscalculation of particle size or no detection.
More than one particle type of higher density (e.g. protein and rubber, steel, glass)	Potential differentiation according to visual appearance (refractive index or shape).	No differentiation possible.

For RMM, the discrimination was very accurate for different types of protein particles and different ratios as long as sufficiently high numbers of particles were detected. The high accuracy of RMM is due to the straightforward categorization of particles and droplets according to buoyant mass. This makes RMM a very robust technique for exactly this task. It needs to be considered that RMM can only discriminate one type of positively buoyant from one type of negatively buoyant particles. Thus, if a sample contains protein particles as well as other particles of higher density than the buffer, e.g., particles shed from filling pumps or rubber stoppers, RMM is not able to discriminate them. Here, methods such as SEM-EDS, FT-IR or Raman microscopy (43) could be used as orthogonal methods to further identify these "non-silicone oil" particles. Furthermore, complexes consisting of both protein and silicone oil can pose a challenge for the technique of RMM: The reported size of those complexes may be incorrect due to the simultaneous influence of both material densities on the density of the complex. As a worst case the complexes might be missed entirely as the higher density of protein is compensated by the lower density of silicone oil, eliminating a clear density difference between particle and formulation. Those complexes might be detectable by MFI (given that they are large enough) as shown for an IgG particle containing silicone oil (22). In our study, only very few of those complexes were observed in MFI, because protein particles and silicone oil droplets were prepared separately to avoid interactions of protein and silicone oil during the particle formation process.

Taken together, the robust detection principle of RMM has brought significant benefit to the field of protein product characterization, especially for the discrimination of silicone oil droplets and protein particles. RMM differentiation is recommended for particles below 2 µm, provided that sufficient particle quantities are detected. MFI differentiation is recommended above 2 µm, preferably using a customized filter. In order to cover a size range as broad as possible, both techniques should be applied in parallel for a comprehensive analysis of samples potentially containing silicone oil droplets and protein particles in the size range from 500 nm to 70 µm.

References

1. Narhi LO, Schmit J, Bechtold-Peters K, Sharma D. Classification of protein aggregates. J Pharm Sci. 2012 Feb;101(2):493–8.

2. Carpenter J, Cherney B, Lubinecki A, Ma S, Marszal E, Mire-Sluis A, et al. Meeting report on protein particles and immunogenicity of therapeutic proteins: filling in the gaps in risk evaluation and mitigation. Biologicals. 2010 Sep;38(5):602–11.

3. Rosenberg AS. Effects of protein aggregates: an immunologic perspective. AAPS J. 2006 Jan;8(3):E501–7.

4. Chi EY, Krishnan S, Randolph TW, Carpenter JF. Physical stability of proteins in aqueous solution: mechanism and driving forces in nonnative protein aggregation. Pharm Res. 2003 Sep;20(9):1325–36.

5. USP <788>. Particulate Matter in Injections. In: The United States Pharmacopoeia, National Formulary. 2009.

6. Ph.Eur. 2.9.19. General, particulate contamination: sub-visible particles. In: The European Pharmacopoeia,. 7th ed. 2011.

7. Kirshner LS. Regulatory expectations for analysis of aggregates and particles. In: Colorado Protein Stability Conference. Breckenridge, CO; 2012.

8. Kerwin BA, Akers MJ, Apostol I, Moore-Einsel C, Etter JE, Hess E, et al. Acute and long-term stability studies of deoxy hemoglobin and characterization of ascorbate-induced modifications. J Pharm Sci. 1999 Jan;88(1):79–88.

9. Hawe A, Friess W. Stabilization of a hydrophobic recombinant cytokine by human serum albumin. J Pharm Sci. 2007 Nov;96(11):2987–99.

10. Tyagi AK, Randolph TW, Dong A, Maloney KM, Hitscherich C, Carpenter JF. IgG particle formation during filling pump operation: A case study of heterogeneous nucleation on stainless steel nanoparticles. J Pharm Sci. 2009;98(1):94–104.

11. Freund KB, Laud K, Eandi CM, Spaide RF. Silicone oil droplets following intravitreal injection. Retina. 26(6):701–3.

12. Chantelau E, Berger M. Pollution of insulin with silicone oil, a hazard of disposable plastic syringes. Lancet. 1985;325(8443):1459.

13. Chantelau E, Berger M, Bohlken B. Silicone oil released from disposable insulin syringes. Diabetes Care. 1986;9(6):672–3.

14. Barnard JG, Babcock K, Carpenter JF. Characterization and quantitation of aggregates and particles in interferon-β products: Potential links between product quality attributes and immunogenicity. J Pharm Sci. 2013;102(3):915–28.

15. Felsovalyi F, Janvier S, Jouffray S, Soukiassian H, Mangiagalli P. Silicone-oil-based subvisible particles: Their detection, interactions, and regulation in prefilled container closure systems for biopharmaceuticals. J Pharm Sci. 2012;101(12):4569–83.

16. Thirumangalathu R, Krishnan S, Ricci MS, Brems DN, Randolph TW, Carpenter JF. Silicone oil- and agitation-induced aggregation of a monoclonal antibody in aqueous solution. J Pharm Sci. 2009 Sep;98(9):3167–81.

17. Jones LS, Kaufmann A, Middaugh CR. Silicone oil induced aggregation of proteins. J Pharm Sci. 2005 Apr;94(4):918–27.

18. Ludwig DB, Carpenter JF, Hamel J-B, Randolph TW. Protein adsorption and excipient effects on kinetic stability of silicone oil emulsions. J Pharm Sci. 2010 Apr;99(4):1721–33.

19. Britt KA, Schwartz DK, Wurth C, Mahler HC, Carpenter JF, Randolph TW. Excipient effects on humanized monoclonal antibody interactions with silicone oil emulsions. J Pharm Sci. 2012 Sep 16;101(12):4419–32.

20. Kossovsky N, Heggers JP, Robson MC. Experimental demonstration of the immunogenicity of silicone-protein complexes. J Biomed Mater Res. 1987 Sep;21(9):1125–33.

21. Zölls S, Tantipolphan R, Wiggenhorn M, Winter G, Jiskoot W, Friess W, et al. Particles in therapeutic protein formulations, Part 1: overview of analytical methods. J Pharm Sci. 2012 Mar;101(3):914–35.

22. Wuchner K, Büchler J, Spycher R, Dalmonte P, Volkin DB. Development of a microflow digital imaging assay to characterize protein particulates during storage of a high concentration IgG1 monoclonal antibody formulation. J Pharm Sci. 2010 Aug;99(8):3343–61.

23. Lankers M, Munhall J, Valet O. Differentiation between foreign particulate matter and silicone oil induced protein aggregation in drug solutions by automated Raman spectroscopy. Microsc Microanal. 2008 Aug 3;14(S2):1612–3.

24. Fraunhofer W, Winter G. The use of asymmetrical flow field-flow fractionation in pharmaceutics and biopharmaceutics. Eur J Pharm Biopharm. 2004 Sep;58(2):369–83.

25. Ludwig DB, Trotter JT, Gabrielson JP, Carpenter JF, Randolph TW. Flow cytometry: a promising technique for the study of silicone oil-induced particulate formation in protein formulations. Anal Biochem. 2011 Mar 15;410(2):191–9.

26. Sharma DK, King D, Oma P, Merchant C. Micro-flow imaging: flow microscopy applied to sub-visible particulate analysis in protein formulations. AAPS J. 2010 Sep;12(3):455–64.

27. Sharma DK, Oma P, Pollo MJ, Sukumar M. Quantification and characterization of subvisible proteinaceous particles in opalescent mAb formulations using micro-flow imaging. J Pharm Sci. 2010 Jun;99(6):2628–42.

28. Demeule B, Messick S, Shire SJ, Liu J. Characterization of particles in protein solutions: reaching the limits of current technologies. AAPS J. 2010 Dec;12(4):708–15.

29. Liu L, Ammar DA, Ross LA, Mandava N, Kahook MY, Carpenter JF. Silicone oil microdroplets and protein aggregates in repackaged bevacizumab and ranibizumab: effects of long-term storage and product mishandling. Invest Ophthalmol Vis Sci. 2011 Feb;52(2):1023–34.

30. Sharma D, Oma P, Krishnan S. Silicone Microdroplets in Protein Formulations - Detection and Enumeration. Pharm Technol. 2009;33(4):74–9.

31. Strehl R, Rombach-Riegraf V, Diez M, Egodage K, Bluemel M, Jeschke M, et al. Discrimination between silicone oil droplets and protein aggregates in biopharmaceuticals: a novel multiparametric image filter for sub-visible particles in microflow imaging analysis. Pharm Res. 2012 Feb;29(2):594–602.

32. Burg TP, Godin M, Knudsen SM, Shen W, Carlson G, Foster JS, et al. Weighing of biomolecules, single cells and single nanoparticles in fluid. Nature. 2007 Apr 26;446(7139):1066–9.

33. Dextras P, Burg TP, Manalis SR. Integrated measurement of the mass and surface charge of discrete microparticles using a suspended microchannel resonator. Anal Chem. 2009 Jun 1;81(11):4517–23.

34. Rosenberg AS, Verthelyi D, Cherney BW. Managing uncertainty: A perspective on risk pertaining to product quality attributes as they bear on immunogenicity of therapeutic proteins. J Pharm Sci. 2012;101(10):3560–7.

35. Patel AR, Lau D, Liu J. Quantification and Characterization of Micrometer and Submicrometer Subvisible Particles in Protein Therapeutics by Use of a Suspended Microchannel Resonator. Anal Chem. 2012 Jul 13;84(15):6833–40.

36. Ph.Eur. 3.1.8. Silicone oil used as a lubricant. In: The European Pharmacopoeia,. 7th ed. 2010.

37. Fischer H, Polikarpov I, Craievich AF. Average protein density is a molecular-weight-dependent function. Protein Sci. 2004 Oct;13(10):2825–8.

38. Majumdar S, Ford BM, Mar KD, Sullivan VJ, Ulrich RG, D'souza AJM. Evaluation of the effect of syringe surfaces on protein formulations. J Pharm Sci. 2011 Jul;100(7):2563–73.

39. Chantelau E. Silicone oil contamination of insulin. Diabet Med. 1989 Apr;6(3):278.

40. Pedersen JS. Statistical evaluation of MFI dataset quality for high-throughput analysis. In: Protein Simple User Meeting, Basle, Switzerland. 2012.

41. Zölls S, Gregoritza M, Tantipolphan R, Wiggenhorn M, Winter G, Friess W, et al. How subvisible particles become invisible-relevance of the refractive index for protein particle analysis. J Pharm Sci. 2013 Mar 5;102(5):1434–46.

42. Ripple DC, Wayment JR, Carrier MJ. Standards for the Optical Detection of Protein Particles. Am Pharm Rev. 2011;(4):90–6.

43. Cao X, Masatani P, Torraca G, Wen ZQ. Identification of a mixed microparticle by combined microspectroscopic techniques: A real forensic case study in the biopharmaceutical industry. Appl Spectrosc. 2010;64(8):895–900.

Supplementary information

Table S1: Total particle and silicone oil droplet concentrations of expired marketed products in prefilled syringes determined by RMM.

Product	Total particle concentration (> 0.5 µm)	Identified as silicone oil droplets (> 0.5 µm)
etanercept		
lot 32411, exp.09/2009	1.50 x 106	1.46 x 106
lot 31576, exp.12/2008	3.25 x 106	1.68 x 106
adalimumab		
lot 430989A04, exp.02/2008	1.74 x 106	1.61 x 106
lot 292209A05, exp.10/2006	2.01 x 106	1.94 x 106

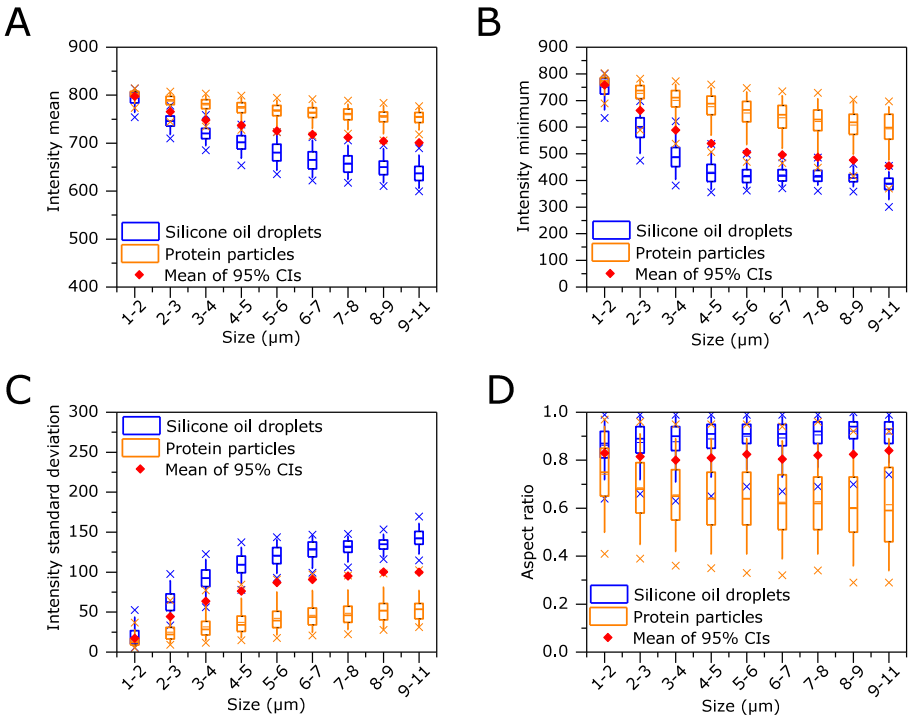

Figure S1: Distribution of the MFI particle parameters A) intensity mean, B) intensity minimum, C) intensity standard deviation and D) aspect ratio for individual samples of silicone oil droplets and protein particles (heat-stressed Rituximab). Box plots show 25/75% (box) and 5/95% percentiles (whisker) as well as minimum and maximum values (X). The mean values of the 95% confidence intervals (CI) were used as a basis to fit the function for the customized filter.

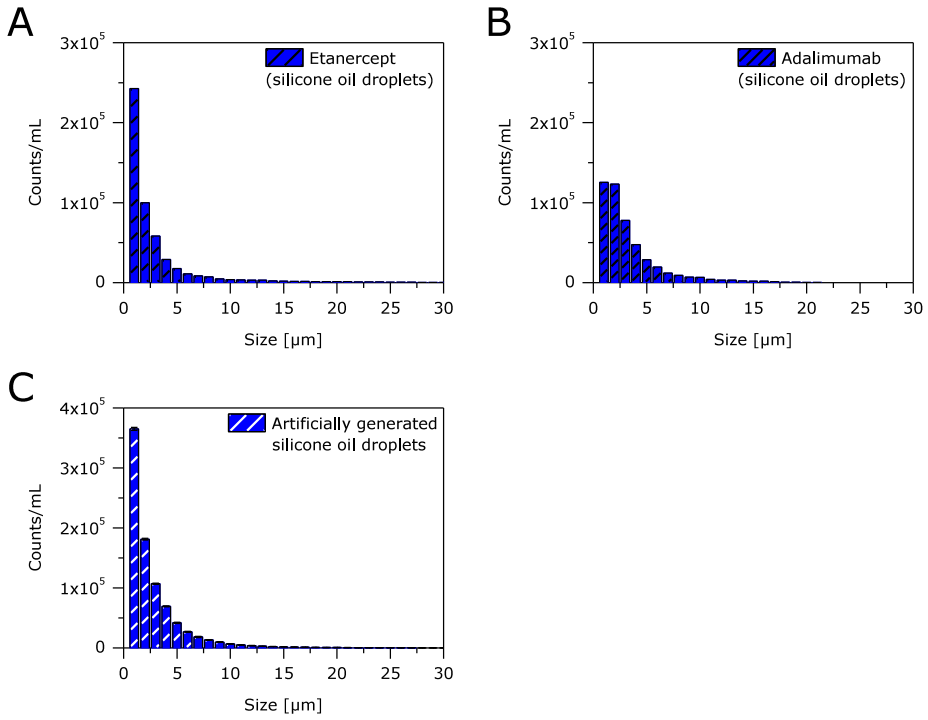

Figure S2: Cumulative size distributions of silicone oil droplets determined by MFI and identified by the "find similar" operation in A) Etanercept prefilled syringes, B) Adalimumab prefilled syringes, C) a sample containing only artificially generated silicone oil droplets. Error bars represent standard deviations from triplicate measurements.

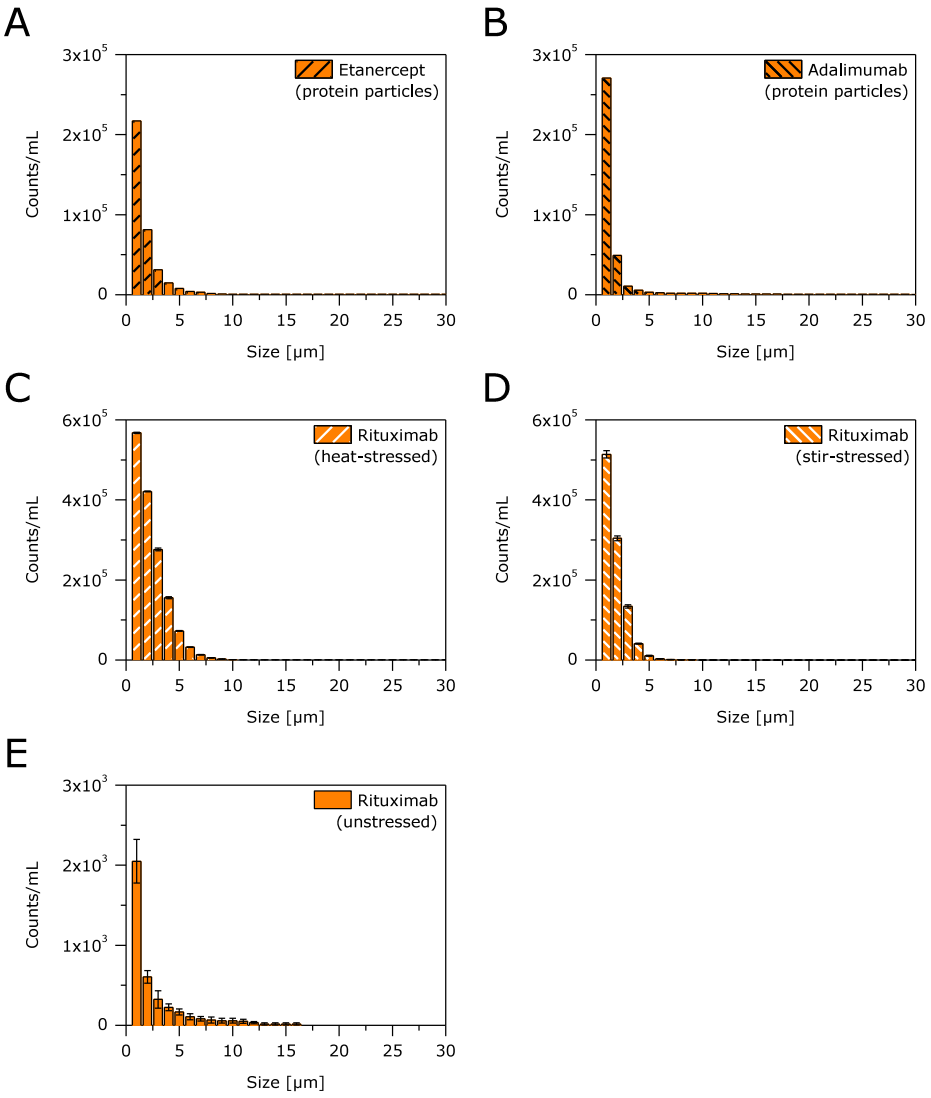

Figure S3: Cumulative size distributions of protein particles determined by MFI and identified by the "find similar" operation for silicone oil droplets (protein particles are identified as the inverse pop ulation) in A) Etanercept prefilled syringes, B) Adalimumab prefilled syringes, C) heat-stressed Rituximab, D) stir-stressed Rituximab, E) unstressed Rituximab. Error bars represent standard deviations from triplicate measurements.

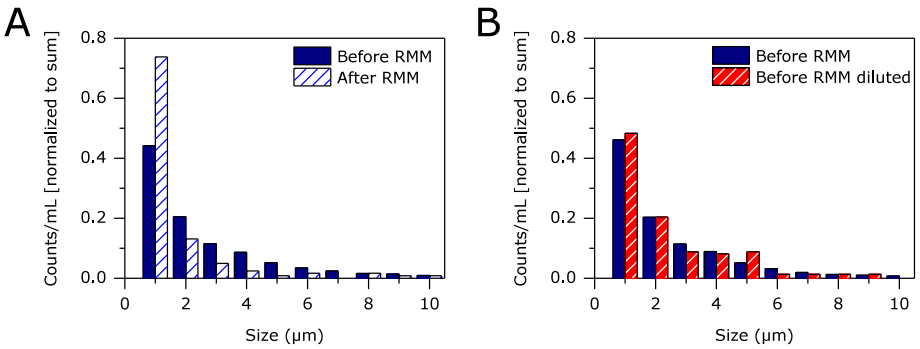

Figure S4: Differential size distribution of a sample containing only silicone oil droplets (0.04% (w/v)) analyzed by MFI, A) before RMM and collected after RMM analysis and B) before and after dilution according to the dilution factor 218 of the sample during RMM analysis. Counts were normalized to the total particle count.

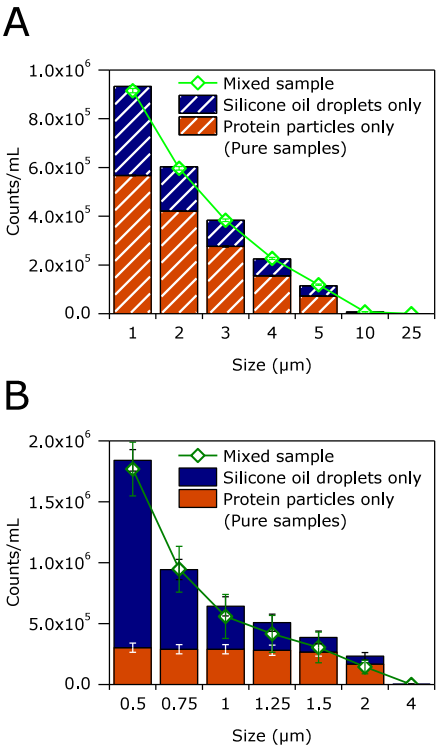

Figure S5: Cumulative counts in individual samples of silicone oil droplets and protein particles (heat-stressed Rituximab) and the corresponding mixture analyzed by A) MFI and B) RMM. Error bars represent standard deviations from triplicate measurements.